93-GT-239

THE AMERICAN SOCIETY OF MECHANICAL ENGINEERS
345 E. 47th St., New York, N.Y. 10017

A THERMAL FATIGUE MODEL FOR PROBABILISTIC LIFETIME STRENGTH OF PROPULSION SYSTEM COMPONENTS

L. Boyce
Associate Professor of Mechanical Engineering
The University of Texas at San Antonio
San Antonio, Texas

C. C. Bast
Graduate Research Assistant
The University of Texas at San Antonio
San Antonio, Texas

ABSTRACT

This paper describes the development of methodology for a probabilistic material strength degradation model, that provides for quantification of uncertainty in the lifetime material strength of structural components of aerospace propulsion systems subjected to a number of diverse random effects. The model has most recently been extended to include thermal fatigue. The discussion of thermal fatigue, in the context of probabilistic material strength degradation, is the central feature of this paper. The methodology, for all effects, is embodied in two computer programs, PROMISS and PROMISC. These programs form a "material resistance" model that may be used in the aerospace structural reliability program, NESSUS or in other applications. A probabilistic material strength degradation model for thermal fatigue and other relevant effects, in the form of a postulated randomized multifactor interaction equation, is used to quantify lifetime material strength. Each multiplicative term in the model has the property that if the current value of an effect equals the ultimate value, then the lifetime strength will be zero. Also, if the current value of an effect equals the reference value, the term equals one and lifetime strength is not affected by that particular effect. Presently, the model includes up to four effects that typically reduce lifetime strength: high temperature, mechanical fatigue, creep and thermal fatigue. Statistical analysis of experimental data for Inconel 718 obtained from the open literature and laboratory reports is also included in the paper. The statistical analysis provided regression parameters for use as the model's empirical material constants, thus calibrating the model specifically for Inconel 718. Model calibration was carried out for four variables, namely, high temperature, mechanical fatigue, creep and thermal fatigue. Finally, using the PROMISS computer program, a sensitivity study was performed with the calibrated random model to illustrate the effects of mechanical fatigue, creep and thermal fatigue, at about 1000 °F, upon random lifetime strength.

NOMENCLATURE

A_i	current value of the i^{th} effect
A_{iU}	ultimate value of the i^{th} effect
A_{iO}	reference value of the i^{th} effect
a_i	i^{th} value of the empirical material constant
b	fatigue strength exponent
c	fatigue ductility exponent
E	modulus of elasticity
K_t	stress concentration factor
K'	cyclic strength coefficient
n	number of effect product terms in the model
n'	cyclic strain hardening exponent
N	current value of mechanical fatigue cycles
N'	current value of thermal fatigue cycles
N'_F	number of thermal fatigue cycles to failure
$2N'_F$	number of thermal fatigue reversals to failure
N_U	ultimate value of mechanical fatigue cycles

Presented at the International Gas Turbine and Aeroengine Congress and Exposition
Cincinnati, Ohio — May 24–27, 1993

N'_U	ultimate value of thermal fatigue cycles
N_O	reference value of mechanical fatigue cycles
N'_O	reference value of thermal fatigue cycles
q	material constant for temperature
R^2	coefficient of determination
s	material constant for mechanical fatigue cycles
S	current value of material strength
S_O	reference value of material strength
T	current value of temperature
T_C	creep threshold temperature
T_M	ultimate (melting) value of temperature
T_O	reference value of temperature
t	current value of creep time
t_U	ultimate value of creep time
t_O	reference value of creep time
u	material constant for thermal fatigue cycles
v	material constant for creep time
$\Delta\varepsilon_P/2$	plastic strain amplitude
$\Delta\varepsilon_T/2$	total strain amplitude
$\Delta\sigma/2$	stress amplitude
ε'_F	fatigue ductility coefficient
σ'_F	fatigue strength coefficient

INTRODUCTION

Previously, a general material behavior degradation model for composite materials, subjected to a number of diverse effects or variables, was postulated to predict mechanical and thermal material properties (Chamis, 1984; Chamis and Hopkins, 1985; Hopkins and Chamis, 1985; Hopkins, 1984). The resulting multifactor interaction equation summarizes a proposed composite micromechanics theory and has been used to predict material properties for a unidirectional fiber-reinforced lamina based on the corresponding properties of the constituent materials.

Recently, the equation has been modified to predict the lifetime strength of a single constituent material due to "n" diverse effects or variables (Boyce and Chamis, 1989; Boyce et al, 1991; Boyce and Bast, 1992). These effects could include variables such as high temperature, creep, mechanical fatigue, thermal fatigue, corrosion or even radiation attack. For most of these variables, strength has been observed to decrease with an increase in the variable (Flinn and Trojan, 1990). It is the purpose of the present work to extend the modified multifactor interaction equation to account for the degradation of lifetime strength due to thermal fatigue. The general form of the postulated equation is

$$\frac{S}{S_O} = \prod_{i=1}^{n} \left[\frac{A_{iU} - A_i}{A_{iU} - A_{iO}}\right]^{a_i}, \qquad (1)$$

where A_i, A_{iU} and A_{iO} are the current, ultimate and reference values, respectively, of a particular effect; a_i is the value of an empirical material constant for the i^{th} product terms of variables in the model; S and S_O are the current and reference values of material strength. Each term has the property that if the current value equals the ultimate value, the lifetime strength will be zero. Also, if the current value equals the reference value, the term equals one and strength is not affected by that variable.

This deterministic material strength degradation model may be calibrated by appropriately curve-fitted least squares multiple linear regression of experimental data (Ross, 1987), perhaps supplemented by expert opinion. Ideally, experimental data giving the relationship between effects and strength is obtained. For example, data for just one effect could be plotted on log-log paper. A good fit for the data may be obtained by linear regression. This is shown schematically in Figure 1. Dropping the subscript "i" for a single variable, the postulated equation is obtained by noting the linear relation between log S and log $[(A_U - A_O)/(A_U - A)]$, as follows:

$$\log S = - a \log\left[\frac{A_U - A_O}{A_U - A}\right] + \log S_O$$

$$\log S - \log S_O = - a \log\left[\frac{A_U - A_O}{A_U - A}\right]$$

$$\log \frac{S}{S_O} = - a \log\left[\frac{A_U - A_O}{A_U - A}\right]$$

$$\frac{S}{S_O} = \left[\frac{A_U - A_O}{A_U - A}\right]^{-a} \qquad (2a)$$

or,

$$\frac{S}{S_O} = \left[\frac{A_U - A}{A_U - A_O}\right]^{a}. \qquad (2b)$$

Equation (2a), above, is for a variable that lowers strength. Note that if a variable raises

strength the exponent, a, in equation (2a) is negative.

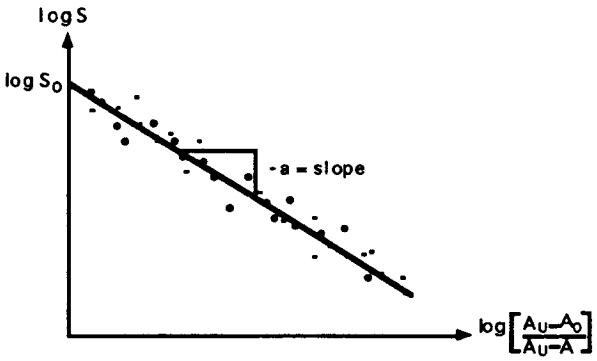

Fig. 1 Schematic of Data Illustrating the Effect of One Primitive Variable on Strength.

This general material strength degradation model, given by equation (1), may be used to estimate the lifetime strength, S/S_O, of an aerospace propulsion system component operating under the influence of a number of diverse effects or variables. The probabilistic treatment of this model includes randomizing the deterministic multifactor interaction equation, performing probabilistic analysis by simulation and generating a probability density function (p.d.f.) estimate for lifetime strength, using the non-parametric method of maximum penalized likelihood (Scott, 1976; Siddall, 1982). Integration of the probability density function yields the cumulative distribution function (c.d.f.) from which probability statements regarding lifetime strength may be made. This probabilistic material strength degradation model, therefore, predicts the random lifetime strength of an aerospace propulsion component subjected to a number of diverse random effects.

The general probabilistic material strength degradation model, given by equation (1), is embodied in two FORTRAN programs, PROMISS (Probabilistic Material Strength Simulator) and PROMISC (Probabilistic Material Strength Calibrator) (Boyce et al, 1991). PROMISS calculates the random lifetime strength of an aerospace propulsion component subjected to as many as eighteen diverse random effects. Results are presented in the form of probability density functions and cumulative distribution functions of lifetime strength, S/S_O. PROMISC calibrates the model by calculating the values of the empirical material constants, a_i.

STRENGTH DEGRADATION MODELS FOR HIGH TEMPERATURE, MECHANICAL FATIGUE AND CREEP FOR INCONEL 718

Prior to extending the multifactor interaction equation for material strength degradation to thermal fatigue, the model was modified for high temperature, mechanical fatigue and creep. When modified for these three effects it became,

$$\frac{S}{S_O} = \left[\frac{T_M - T_O}{T_M - T}\right]^{-q} \left[\frac{N_U - N_O}{N_U - N}\right]^{-s} \left[\frac{t_U - t_O}{t_U - t}\right]^{-v}, \quad (3)$$

where T_M is the ultimate or melting temperature of the material, T_O is a reference or room temperature, T is the current temperature, N_U is the ultimate number of cycles (for which fatigue strength is very small), N_O is a reference number of cycles (for which fatigue strength is very large), N is the current number of cycles the material has undergone, t_U is the ultimate number of creep hours (for which rupture strength is very small), t_O is a reference number of creep hours (for which rupture strength is very large) and t is the current number of creep hours. Also q, s and v are empirical material parameters, one for each effect, that represent the slope of a straight line fit of the data on log-log paper.

Appropriate values for the ultimate and reference quantities had to be selected prior to calibration of the multifactor interaction equation for Inconel 718. For example, for Inconel 718 the average melting temperature, $T_M = 2369\ ^\circ F$, was a logical choice for the ultimate temperature value. Hence, after appropriate selection of the ultimate and reference values for each of the three effects, equation (3) became,

$$\frac{S}{S_O} = \left[\frac{2369 - 75}{2369 - T}\right]^{-q} \left[\frac{10^{10} - 0.5}{10^{10} - N}\right]^{-s} \left[\frac{10^6 - 0.25}{10^6 - t}\right]^{-v}. \quad (4a)$$

When the current value and the reference value are small compared to the ultimate value, the log of each value is used. Experience has shown that this transformation increases the sensitivity of an effect to the data used within it. Also, it usually results in better statistical

fits of the data for linear regression. Hence, equation (4a) becomes,

$$\frac{S}{S_O} = \left[\frac{2369 - 75}{2369 - T}\right]^{-q} \left[\frac{\log 10^{10} - \log 0.5}{\log 10^{10} - \log N}\right]^{-s} \left[\frac{\log 10^{6} - \log 0.25}{\log 10^{6} - \log t}\right]^{-v} . \quad (4b)$$

The ultimate and reference values in equation (4a) and (4b) became model parameters or constraints for the multifactor interaction equation when modified for Inconel 718. Figure 2 illustrates these model parameters for equation (4a) graphically, wherein each axis represents an effect or primitive variable. Note also an additional constraint in Figure 2, namely the creep threshold temperature, T_C = 900 °F. Although this constraint is not explicitly built into the multifactor interaction equation, it may be taken into account indirectly. This is accomplished by not including the creep effect whenever the current value of temperature, T, is below 900 °F. Similarily, when data for mechanical fatigue and/or creep result from tests conducted at high temperatures, the temperature effect is not included. Note that the empirical material parameters, q, s and v had to be determined from regression analysis of actual experimental data.

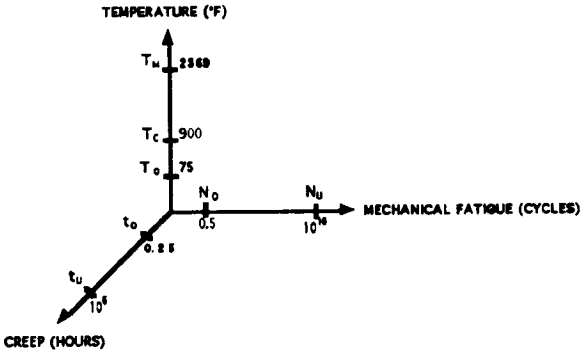

Fig. 2 Model Parameters for Inconel 718 for Temperature, Mechanical Fatigue and Creep.

STRENGTH DEGRADATION MODEL FOR THERMAL FATIGUE

Thermal fatigue has been extensively discussed in the literature (Collins, 1981; Kuwabara and Kitamura, 1983; Swindelman and Douglas, 1959). The general model for the thermal fatigue effect uses stress-life (σ-N) data obtained from experimental strain-life (ε-N) data. Total strain amplitude data and plastic strain amplitude data were used to construct a strain-life curve (Kuwabara and Kitamura, 1983). The plastic portion of the curve may be represented by the following power law function:

$$\frac{\Delta\varepsilon_P}{2} = \varepsilon'_F (2N'_F)^c , \quad (5)$$

where $\Delta\varepsilon_P/2$ is the plastic strain amplitude and $2N'_F$ are the reversals to failure. A power law regression analysis of the data yields two thermal fatigue properties, namely, the fatigue ductility coefficient, ε'_F, and the fatigue ductility exponent, c. Regression statistics, such as the coefficient of determination, R^2, can indicate whether or not a power law representation of the relationship between plastic strain amplitude and reversals to failure is satisfactory.

Stress amplitude, $\Delta\sigma/2$, can be calculated using the modulus of elasticity, E, and the total and plastic strain amplitudes, $\Delta\varepsilon_T/2$ and $\Delta\varepsilon_P/2$, respectively, by the following equation:

$$\frac{\Delta\sigma}{2} = E\left[\frac{\Delta\varepsilon_T}{2} - \frac{\Delta\varepsilon_P}{2}\right] . \quad (6)$$

When the resulting stress amplitude is plotted against plastic strain amplitude the cyclic stress-strain plot results. Again, a power law function may be satisfactory for expressing the cyclic stress-strain relationship. The following power law function may be used:

$$\frac{\Delta\sigma}{2} = K'\left(\frac{\Delta\varepsilon_P}{2}\right)^{n'} , \quad (7)$$

where K' is the cyclic strength coefficient and n' is the cyclic strain hardening exponent, two additional thermal fatigue properties.

When the stress amplitude is plotted against reversals to failure, the stress-life plot results. The following power law function may be used to approximate this relationship:

$$\frac{\Delta\sigma}{2} = \sigma'_F (2N_F)^b , \quad (8)$$

where σ'_F is the fatigue strength coefficient and b is the fatigue strength exponent. These final two properties complete the set of thermal fatigue material properties.

With the ordinate now expressed in stress units (psi), this fourth effect can be added to the material strength degradation model depicted by equations (3) and (4). This effect will have the form,

$$\left[\frac{N'_U - N'_O}{N'_U - N'}\right]^{-u} = \left[\frac{10^5 - 0.5}{10^5 - N'}\right]^{-u},$$

where $N'_U = 10^5$ is the ultimate number of thermal cycles (for which thermal fatigue strength is very small), $N'_O = 0.5$ is the selected reference number of thermal cycles (for which thermal fatigue strength is very large), N' is the current number of thermal cycles the material has undergone and u is an empirical material constant found from a power law regression of the data. Thus, equations (3) and (4) will now include four terms, one for each effect, as shown below:

$$\frac{S}{So} = \left[\frac{T_M - T_O}{T_M - T}\right]^{-q}\left[\frac{N_U - N_O}{N_U - N}\right]^{-s}\left[\frac{t_U - t_O}{t_U - t}\right]^{-v}\left[\frac{N'_U - N'_O}{N'_U - N'}\right]^{-u}, \quad (9)$$

$$\frac{S}{So} = \left[\frac{2369 - 75}{2369 - T}\right]^{-q}\left[\frac{10^{10} - 0.5}{10^{10} - N}\right]^{-s}\left[\frac{10^6 - 0.25}{10^6 - t}\right]^{-v}\left[\frac{10^5 - 0.5}{10^5 - N'}\right]^{-u} \quad (10)$$

EXPERIMENTAL MATERIAL DATA FOR INCONEL 718

Calibration of the multifactor interaction equation for Inconel 718 requires the collection of experimental data, and subsequent statistical analysis of the data, to determine the empirical material constants, a_i. A computerized literature search of Inconel 718, a nickel-base superalloy, was conducted to obtain existing experimental data on various material properties. Data on high temperature tensile strength, mechanical fatigue strength, creep rupture strength and thermal fatigue strength properties were obtained for Inconel 718 (Barker et al, 1970; Cullen and Freeman, 1985; INCONEL Alloy 718, 1986; Kuwabara and Kitamura, 1983; Sims et al, 1987; Swindelman and Douglas, 1959). This data resulted from tests done on various hot worked specimens, including sheets of Inconel 718, as well as, hot rolled bars of the superalloy.

Thermal fatigue data results from both low cycle mechanical fatigue tests, as well as, thermal fatigue tests. Low cycle fatigue produces cumulative material damage and ultimate failure in a component by the cyclic application of strains that extend into the plastic range. Failure typically occurs under 10^5 cycles. Low cycle fatigue is often produced mechanically under isothermal conditions. However, machine components may also be subjected to low cycle fatigue due to a cyclic thermal field. These cyclic temperature changes produce thermal expansions and contractions that, if constrained, produce cyclic strains and stresses. These thermally induced stresses and strains result in fatigue failure in the same manner as those produced mechanically.

Low cycle fatigue tests, comparing both mechanically strain cycled specimens at constant elevated temperatures and thermally cycled constrained specimens, have been conducted on stainless steel (Collins, 1981) and Inconel (Swindelman and Douglas, 1959). Results are typically plotted as plastic strain range versus cycles to failure. For stainless steel, these plots show that for equal values of plastic strain range the number of cycles to failure was much *less* for the thermally cycled specimens than for the mechanically cycled ones. To bring the thermal fatigue test results into coincidence with the isothermal mechanical fatigue test results, requires the multiplication of the strain, for any number of cycles to failure, by a factor of approximately 2.5 (Collins, 1981). Inconel, however, responds to mechanically produced plastic strain in the *same* manner as it responds to thermally produced plastic strain at elevated temperatures (Swindelman and Douglas, 1959). Thus, the Inconel test results provide a means for utilizing mechanically cycled data to build a thermal fatigue model for Inconel 718.

As previously mentioned, the general model for the thermal fatigue effect uses stress-life (s-N) data obtained from experimental strain-life (e-N) data. The thermal fatigue data presented in Table 1 and displayed as the strain-life curves in Figure 3, resulted from thermomechanical fatigue testing between a minimum temperature of 600 °F and a maximum temperature of 1200 °F, with a mean temperature of approximately 900 °F

(Kuwabara and Kitamura, 1983). The temperature and strain were computer-controlled by the same triangular waveform with in-phase cycling at a frequency of 0.0056 Hz. Using a value of $E = 25 \times 10^6$ psi for the modulus of elasticity for Inconel 718 at 900 °F (INCONEL Alloy 718, 1986), the stress amplitude can be calculated from equation (6). Hence, stress amplitude is plotted against plastic strain amplitude to produce the cyclic stress-strain curve shown in Figure 4. Using the power law regression techniques (Bannantine, 1990) indicated in equations (5), (7), and (8), and the data from Table 1, the thermal fatigue properties for Inconel 718 can be calculated. These material properties are displayed in Table 2 and indicated graphically, along with their coefficient of determination, R^2, in Figures 5, 6, and 7.

Table 1 Thermal Fatigue Data for Inconel 718

Cycles to Failure N'_F	Total Strain Amplitude, $\Delta\varepsilon_T/2$	Plastic Strain Amplitude, $\Delta\varepsilon_P/2$	Stress Amplitude, $\Delta\sigma/2$ (psi)
45	0.0100	0.0050	126,500
140	0.0075	0.0029	116,380
750	0.0050	0.0011	98,670
9750	0.0040	0.0003	93,610

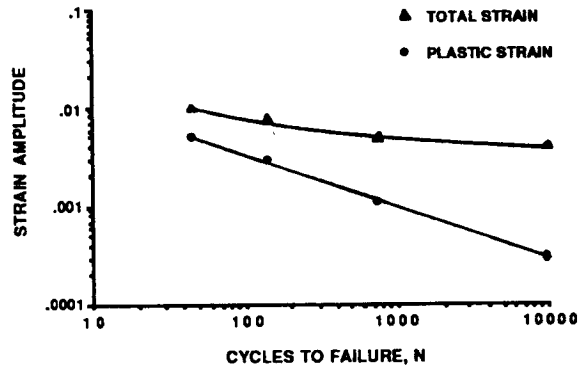

Fig. 3 Strain-life Curve for Inconel 718.

Table 2 Thermal Fatigue Material Properties for Inconel 718

Fatigue Ductility Coefficient, ε'_F	0.0545
Fatigue Ductility Exponent, c	-0.5279
Cyclic Strength Coefficient, K'	219,584 psi
Cyclic Strain Hardening Exponent, n'	0.1089
Fatigue Strength Coefficient, σ'_F	159,625 psi
Fatigue Strength Exponent, b	-0.0572

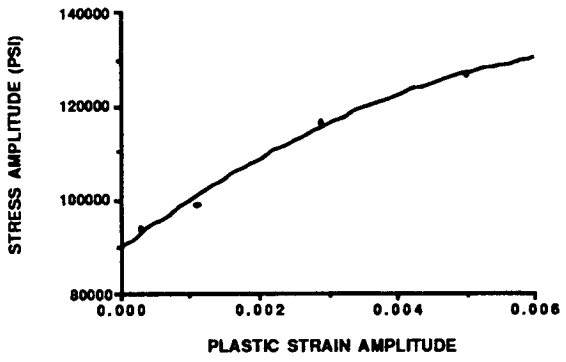

Fig. 4 Cyclic Stress-strain Curve for Inconel 718.

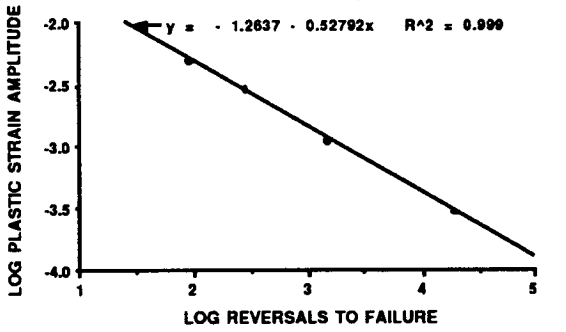

Fig. 5 Regression of Equation (5) Data Yielding Fatigue Ductility Coefficient, ε'_F, and Fatigue Ductility Exponent, c.

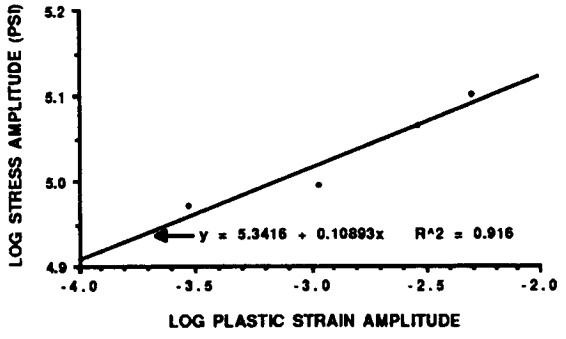

Fig. 6 Regression of Equation (7) Data Yielding Cyclic Strength Coefficient, K', and Cyclic Strain Hardening Exponent, n'.

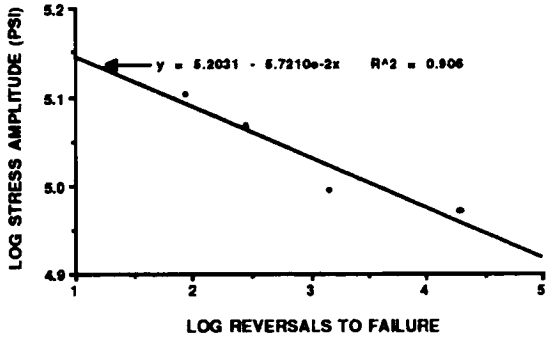

Fig. 7 Regression of Equation (8) Yielding Fatigue Strength Coefficient, σ'_F and Fatigue Strength Exponent, b.

The Inconel 718 data for high temperature, mechanical fatigue, creep and thermal fatigue has been plotted in the same form as that used in the multifactor interaction equation in PROMISS and PROMISC. Figure 8 shows the effect of temperature on yield strength for Inconel 718. As expected, the yield strength of the material decreases as the temperature increases. The data displayed in Figure 9 shows the effect of mechanical fatigue cycles on fatigue strength for Inconel 718 for given test temperatures. As expected, the fatigue strength of the material decreases as the number of cycles increases. The data displayed in Figure 10 shows the effect of creep time on rupture strength for Inconel 718 for given test temperatures. Once again, the strength of the material decreases as the variable, in this case time, increases. Figures 11 shows the effect of thermal fatigue cycles on stress amplitude at failure (i.e., thermal fatigue strength) for Inconel 718 for a mean thermal cycling temperature of 900 °F. As expected, the thermal fatigue strength of the material decreases as the number of cycles increases.

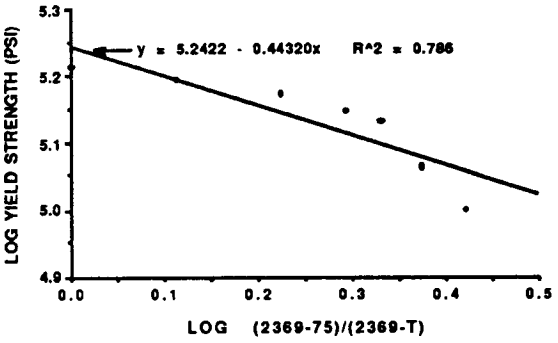

Fig. 8 Effect of Temperature (°F) on Yield Strength for Inconel 718. (Log-Log Plot with Linear Regression)

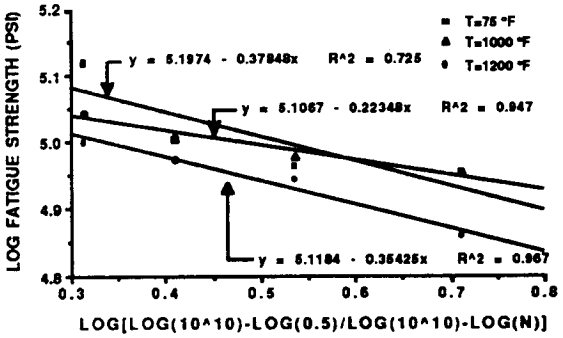

Fig. 9 Effect of Mechanical Fatigue (Cycles) on Fatigue Strength for Inconel 718. (Log-Log Plot with Linear Regression)

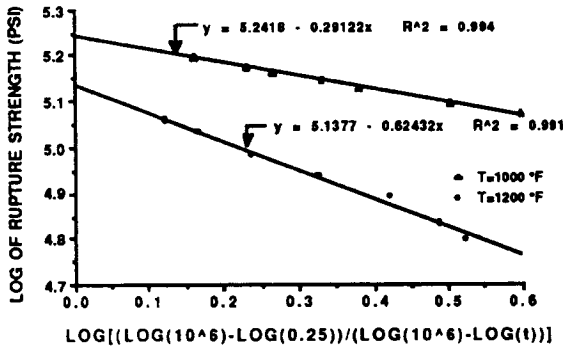

Fig. 10 Effect of Creep Time (Hours) on Rupture Strength for Inconel 718. (Log-Log Plot with Linear Regression)

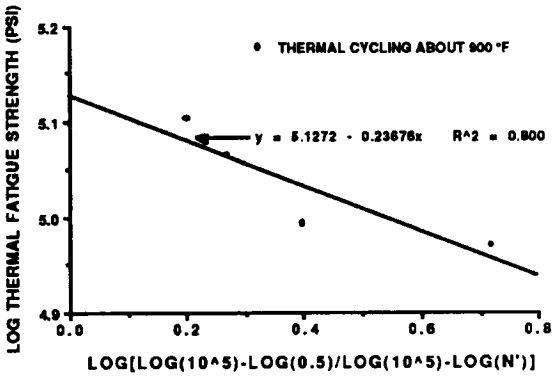

Fig. 11 Effect of Thermal Fatigue (Cycles) on Fatigue Strength for Inconel 718. (Log-Log Plot with Linear Regression)

As seen in Figures 8, 9, 10 and 11, linear regression of the data for temperature, mechanical fatigue, creep and thermal fatigue, respectively, produces first estimates of the empirical material constants, namely, q, s, v and u. The estimated values of these empirical material constants are given by the slopes of the linear fits.

PROBABILISTIC LIFETIME STRENGTH SENSITIVITY STUDY FOR MECHANICAL FATIGUE, CREEP AND THERMAL FATIGUE

Using the probabilistic material strength degradation model embodied in PROMISS, a lifetime strength sensitivity study was conducted. Three effects were included in this study, mechanical fatigue, creep and thermal fatigue. The temperature effect was not included since mechanical and thermal fatigue and creep data *at 1000 °F* were used (see Discussion section). The multifactor interaction equation for material strength degradation, given by equations (9) and (10), when modified for mechanical fatigue, creep and thermal fatigue effects only, becomes,

$$\frac{S}{S_O} = \left[\frac{10^{10} - 0.5}{10^{10} - N}\right]^{-s} \left[\frac{10^{6} - 0.25}{10^{6} - t}\right]^{-v} \left[\frac{10^{5} - 0.5}{10^{5} - N'}\right]^{-u} \quad (11)$$

The empirical material constants for these three effects, namely s, v, and u, as determined from regression analysis of the experimental data, were used to calibrate the model. NASA Lewis Research Center expert opinion and engineering judgment supplied other input values. Typical sets of input values for the PROMISS model represented by equation (11) are given in Tables 3, 4 and 5. For example, Table 3 shows PROMISS input data for a temperature of 1000 °F, a current value of $2.5x10^5$ mechanical fatigue cycles (entered as the log of $2.5x10^5$ or 5.398), a current value of 1000 creep hours (entered as the log of 1000 or 3.0), and a current value of 2000 thermal fatigue cycles (entered as the log of 2000 or 3.301). As seen in Tables 4 and 5, the above mentioned current values remain the same with the exception of the current value of mechanical fatigue cycles. In Tables 4 and 5 the current value of mechanical fatigue cycles has been increased to $1.0x10^6$ (entered as the log of $1.0x10^6$ or 6.0) and $1.75x10^6$ (entered as the log of $1.75x10^6$ or 6.243), respectively. By holding two of the three effects constant, the model's sensitivity towards the third effect, in this case mechanical fatigue cycles, can be determined. The complete set of current values that were used as input data for the sensitivity study are given in Table 6. Notice that the first three rows of the table correspond to the current values listed in Tables 3, 4 and 5, respectively. The next three rows of Table 6 show how the current values of creep hours were varied, while the last three rows show how the current thermal fatigue values were varied. The results of this study, in the form of cumulative distribution functions, are given in Figures 12-14, one figure for each effect. For example, Figure 12 shows the effect of mechanical fatigue cycles on lifetime strength. Note that the c.d.f. shifts to the left, indicating a lowering of lifetime strength for increasing mechanical fatigue cycles. In this manner, PROMISS results, in the form of c.d.f.'s, display the sensitivity of lifetime strength to any effect or variable.

Table 3 Sensitivity study input to PROMISS for Inconel 718; Temperature = 1000 °F and N=$2.5x10^5$ cycles

Effect	Variable Symbol	Units	Distribution Type	Mean	Standard Deviation (Value),	(% of Mean)
Mechanical Fatigue	N_U	log of cycle	Normal	10.0	1.0	10.0
	N	log of cycle	Normal	5.398	0.5398	10.0
	N_O	log of cycle	Normal	- 0.3	- 0.03	10.0
	s	N/A	Normal	0.223	0.0067	3.0
Creep	t_U	log of hours	Normal	6.0	0.3	5.0
	t	log of hours	Normal	3.0	0.15	5.0
	t_O	log of hours	Normal	-0.602	-0.03	5.0
	v	N/A	Normal	0.291	0.0087	3.0
Thermal Fatigue	N'_U	log of cycle	Normal	5.0	0.5	10.0
	N'	log of cycle	Normal	3.301	0.33	10.0
	N'_O	log of cycle	Normal	- 0.3	- 0.03	10.0
	u	N/A	Normal	0.237	0.0071	3.0

Table 4 Sensitivity study input to PROMISS for Inconel 718; Temperature = 1000 °F and N=1.0x10^6 cycles

Effect	Variable Symbol	Units	Distribution Type	Mean	Standard Deviation (Value),	(% of Mean)
Mechanical Fatigue	N_U	log of cycle	Normal	10.0	1.0	10.0
	N	log of cycle	Normal	6.0	0.6	10.0
	N_O	log of cycle	Normal	- 0.3	- 0.03	10.0
	s	N/A	Normal	0.223	0.0067	3.0
Creep	t_U	log of hours	Normal	6.0	0.3	5.0
	t	log of hours	Normal	3.0	0.15	5.0
	t_O	log of hours	Normal	-0.602	-0.03	5.0
	v	N/A	Normal	0.291	0.0087	3.0
Thermal Fatigue	N'_U	log of cycle	Normal	5.0	0.5	10.0
	N'	log of cycle	Normal	3.301	0.33	10.0
	N'_O	log of cycle	Normal	- 0.3	- 0.03	10.0
	u	N/A	Normal	0.237	0.0071	3.0

Table 5 Sensitivity study input to PROMISS for Inconel 718; Temperature = 1000 °F and N=1.75x10^6 cycles

Effect	Variable Symbol	Units	Distribution Type	Mean	Standard Deviation (Value),	(% of Mean)
Mechanical Fatigue	N_U	log of cycle	Normal	10.0	1.0	10.0
	N	log of cycle	Normal	6.243	0.6243	10.0
	N_O	log of cycle	Normal	- 0.3	- 0.03	10.0
	s	N/A	Normal	0.223	0.0067	3.0
Creep	t_U	log of hours	Normal	6.0	0.3	5.0
	t	log of hours	Normal	3.0	0.15	5.0
	t_O	log of hours	Normal	-0.602	-0.03	5.0
	v	N/A	Normal	0.291	0.0087	3.0
Thermal Fatigue	N'_U	log of cycle	Normal	5.0	0.5	10.0
	N'	log of cycle	Normal	3.301	0.33	10.0
	N'_O	log of cycle	Normal	- 0.3	- 0.03	10.0
	u	N/A	Normal	0.237	0.0071	3.0

Table 6 Sensitivity study of probabilistic material strength degradation model using PROMISS.

Mechanical Fatigue (Cycles)	Creep (Hours)	Thermal Fatigue (Cycles)
2.5×10^5	1000	2000
1.0×10^6	1000	2000
1.75×10^6	1000	2000
1.0×10^6	250	2000
1.0×10^6	1000	2000
1.0×10^6	1750	2000
1.0×10^6	1000	500
1.0×10^6	1000	2000
1.0×10^6	1000	3500

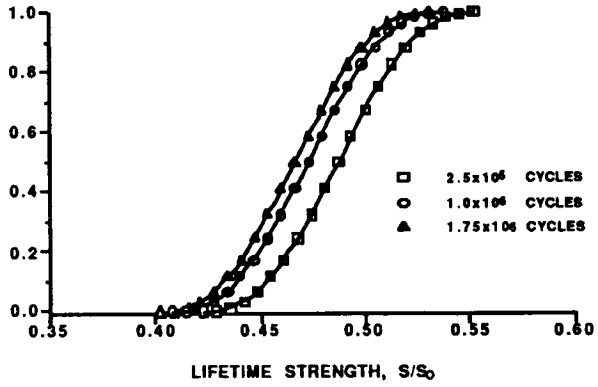

Fig. 12 C.D.F. for Comparison of Various Levels of Uncertainty of Mechanical Fatigue (Cycles) on Probable Strength for Inconel 718 for 2000 Thermal Fatigue Cycles and 1000 Creep Hours at 1000 °F.

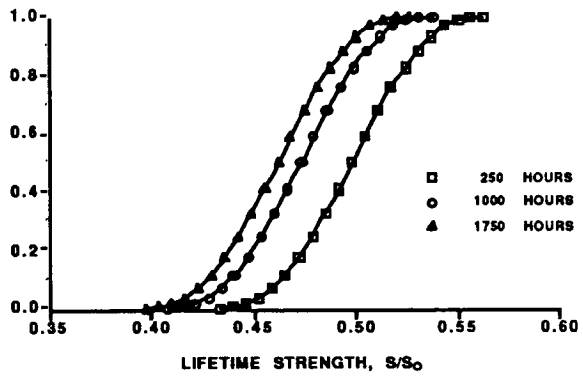

Fig. 13 C.D.F. for Comparison of Various Levels of Uncertainty of Creep Time (Hours) on Probable Strength for Inconel 718 for 1 x 10^6 Mechanical Fatigue Cycles and 2000 Thermal Fatigue Cycles at 1000 °F.

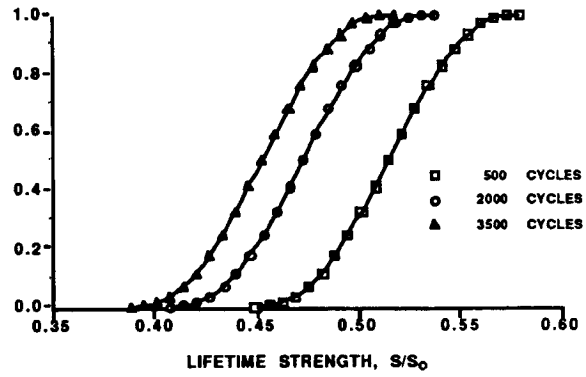

Fig. 14 C.D.F. for Comparison of Various Levels of Uncertainty of Thermal Fatigue (Cycles) on Probable Strength for Inconel 718 for 1 x 10^6 Mechanical Fatigue Cycles and 1000 Creep Hours at 1000 °F.

DISCUSSION

The values of the empirical material constants used to calibrate the model embodied in the PROMISS program are given as mean values in Tables 3-5. These constants were calculated individually for each effect (mechanical fatigue cycles, creep time, and thermal fatigue cycles) as seen by the linear regression fits in Figures 9-11. Although equations (9) and (10) show the multifactor interaction equation for material strength degradation modified for four effects (high temperature, mechanical fatigue cycles, creep time, and thermal fatigue cycles) the sensitivity study presented in Figures 12-14 included only three effects as modeled by equation (11). The

high temperature effect was not included in this particular study due to the fact that the data for the other three effects resulted from tests conducted in a high temperature environment (900 to 1000 °F). Thus, the effect of temperature is inherent in the calculated empirical material constants used to calibrate the model.

The calibration of the model for the multifactor interaction equation utilized the log of each value within each effect, as seen by the x-axis in Figures 9-11. This transformation, attractive when the current value and the reference value are small compared to the ultimate value, was used for the mechanical fatigue, creep and thermal fatigue effects in the sensitivity study. It resulted in a considerable increase in the R^2 values obtained for each of these three effects, over a model without the log transformation. Since R^2, a statistical measure of the goodness of fit, is relatively high, the model well-represented the actual experimental data. Good calibration of the model resulted in realistic lifetime strength values.

Also inherent in the model given by equation (11), is the assumption that the variables are independent and that there are no synergistic effects. This is not actually the case. An attempt has been made to take into account synergistic effects. As previously mentioned, creep effects are not applicable at low temperature values, therefore, they are not included models for sensitivity studies conducted at temperatures below the creep threshold value of 900 °F. In addition, temperature effects are not explicitly included in models for sensitivity studies involving data that results from tests conducted at elevated temperatures. Note in Figures (9) and (10) that the effect of temperature is inherent in the empirical material constants, since their values change according to the test temperature. For example in Figure (10), the value of the empirical material constant for creep increases from a value of 0.29122 at a temperature of 1000 °F to a higher value (steeper slope) of 0.62432 at a temperature of 1200 °F. An increase in the material constant (slope) with an increase in temperature is expected. As Figure (9) indicates, however, the calculated value of the empirical material constant is lower at 1000 °F than at 75 °F. A plausible explanation for this phenomenon is the lack of data points. These values of the empirical material constant for mechanical fatigue are based upon only four actual data points. Thus, for mechanical fatigue, confidence would be increased if a few more actual experimental data points were available.

Simultaneous calibration of the model for all three effects together to build a "combined" or synergistic model to better represent the interdependence of effects may be advantageous. In addition, the subsequent statistical testing of each individual effect, using a synergistic model will assure that it will also model individual effects accurately.

CONCLUSION

A probabilistic material behavior degradation model, applicable to aerospace materials, has been postulated for predicting the random lifetime strength of structural components for aerospace propulsion systems subjected to a number of effects or variables. The model takes the form of a randomized multifactor interaction equation and contains empirical material constants, a_i. Data is available from the open literature for a number of nickel-base superalloys, especially Inconel 718, principally for four individual effects namely, high temperature, mechanical fatigue, creep and thermal fatigue. A model for thermal fatigue has been developed for inclusion into the multifactor interaction equation. Thermal fatigue data for Inconel 718 considers cyclic temperature changes about a mean temperature of 900 °F. Linear regression of this data, together with expert opinion, has resulted in estimates for the empirical material constants through which the model is calibrated.

Thus, a general computational simulation structure is provided for describing the scatter in lifetime strength in terms of probable values for a number of diverse effects or variables. The sensitivity of random lifetime strength to each variable can be ascertained. Probability statements allow improved judgments to be made regarding the likelihood of lifetime strength and hence structural failure of aerospace propulsion system components.

ACKNOWLEDGMENTS

The author gratefully acknowledges the

many helpful conversations and support of Dr. Christos C. Chamis and the NASA Lewis Research Center. Also acknowledged is Mr. Greg Trimble, Texas Space Grant Consortium Undergraduate Research Scholar, of The University of Texas at San Antonio.

REFERENCES

Bannantine, J.A., et. al., Fundamentals of Metal Fatigue Analysis, Prentice Hall, Englewood Cliffs, N.J., 1990, pp. 63 - 66.

Barker, J. F., Ross, E.W. and Radavich, J. F., "Long Time Stability of INCONEL 718," Journal of Metals, Jan. 1970, Vol. 22, p. 32.

Boyce, L. and Bast, C., "Computational Simulation of coupled Material Degradation Processes for Probabilistic Lifetime Strength of Aerospace Materials", L. Boyce, C. Bast, Final Technical Report, NASA CR 1887234, NASA Lewis Research Center, Cleveland, Ohio, Mar. 1992.

Boyce, L. and Chamis, C. C., "Probabilistic Constitutive Relationships for Material Strength Degradation Models," Proceedings of the 30th Structures, Structural Dynamics and Materials Conference, Mobile, AL, April 1989, pp. 1832 - 1839.

Boyce, L., Keating, J., Lovelace, T. and Bast, C., "Probabilistic Lifetime Strength of Aerospace Materials Via Computational Simulation", Final Technical Report, NASA CR 187178, NASA Lewis Research Center, Cleveland, Ohio, Aug. 1991.

Chamis, C. C., "Simplified Composite Micromechanics Equations for Strength, Fracture Toughness, Impact Resistance and Environmental Effects," NASA TM 83696, Jan. 1984.

Chamis, C. C. and Hopkins, D., "Thermoviscoplastic Nonlinear Constitutive Relationships for Structural Analysis of High Temperature Metal Matrix Composites," NASA TM 87291, Nov. 1985.

Collins, J. A., Failure of Materials in Mechanical Design, Wiley-Interscience Publication, John Wiley & Sons, N.Y., 1981, pp. 391 - 393.

Cullen, T. M. and Freeman, J. W., The Mechanical Properties of INCONEL 718 Sheet Alloy at 800°F 1000°F and 1200°F, NASA CR 268, National Aeronautics and Space Administration, Washington, DC, 1985, pp. 20-34.

Flinn, R. A. and Trojan, P. K., Engineering Materials and Their Applications, Houghton Mifflin Co., Dallas, 1990.

Hopkins, D. A., "Nonlinear Analysis for High-Temperature Multilayered Fiber Composite Structures," NASA TM 83754, Aug. 1984.

Hopkins, D. and Chamis, C. C., "A Unique Set of Micromechanics Equations for High Temperature Metal Matrix Composites," NASA TM 87154, Nov. 1985.

INCONEL Alloy 718, Inco Alloys International, Inc., Huntington, WV, 1986, pp. 8-13.

Kuwabara, K., Nitta, A. and Kitamura, T., "Thermal-Mechanical Fatigue Life Prediction in High-Temperature Component Materials for Power Plant," Proceedings of the Advances in Life Prediction Methods Conference, ASME, Albany, N.Y., April, 1983, pp. 131-141.

Ross, S. M., Introduction to Probability and Statistics for Engineers and Scientists, Wiley, New York, 1987, p. 278.

Scott, D.W., "Nonparametric Probability Density Estimation by Optimization Theoretic Techniques," NASA CR-147763, April 1976.

Siddall, J. N., "A Comparison of Several Methods of Probabilistic Modeling," Proceedings of the Computers in Engineering Conference, ASME, Vol. 4, 1982.

Sims, C. T., Stoloff, N.S. and Hagel, W.C., Superalloys II, Wiley, New York, 1987, pp. 581-585, 590-595.

Swindelman, R. W. and Douglas, D.A., "The Failure of Structural Metals Subjected to Strain-Cycling Conditions," Journal of Basic Engineering, ASME transactions, 81, Series D, 1959, pp. 203 -212.